International Journal of Applied Engineering Research ISSN 0973-4562 Volume 10, Number 15 (2015) pp 35918-35926


# A Research On The Aerodynamics And Dynamics Of A Low-Sized Tethered Aerostat Of A Hybrid Design

**Sabir Magomed-Kadievich Bakmaev[1] Gregory Victorovich Tsepilov[1] Ilya Sergeevich Vorontsov[2] Valery Victorovich Ivanov[1]**

*[1]"TECHNOCOMPLEKT" Closed joint-stock company*
*141981, the Moscow region, Dubna, Shkolnaya st., 10A*
*[2]Dubna International University*
*141980, the Moscow region, Dubna, Universitetskaya st., 19*

In the following article, a design of a low-volume tethered aerostatic system is examined, that is intended for meteorology observations at the altitudes up to 1000 meters.
An original aerodynamic configuration of the machine has been designed, which utilizes wings as a source of additional lift (a hybrid design). This approach allows to effectively maintain the required height of flight in windy weather, in contrast to classic tethered balloons.
The paper presents the aerodynamic characteristics of the machine (dependent on the angles of attack and glide), which were obtained by computing that utilized the three dimensional numerical modeling within the framework of the solutions of the Navier-Stocks equations, averaged by the Reynolds method.
We have devised a two-mode onboard control system. In the mode of stabilizing the machine's angular position, the required values of bank and pitch angles are maintained, which is crucial to the proper functioning of the target equipment. The mode of height stabilizing prevents the unacceptable loss of height in downward air currents.
The required degree of steadiness in the axis of the course is achieved by introducing selection options for the position of the tether's attachment point.
The article presents the results of a simulation of the aerostat's flight dynamics. The dynamic impact of the machine on the tether cable is analyzed. The critical speed of the machine is defined, with regard to the tether's durability. It is demonstrated that the machine meets the desired requirements.

**Keywords**: a tethered balloon, a hybrid aerostat, the aerodynamics of the aerostat, the dynamics of the aerostat, the automatic control system

## Introduction

Tethered aerostat systems (TAS) are currently becoming more and more widely adopted, they serve for the surveillance over the airspace, terrain, receiving and transmitting signals, and so on [1].
The aerodynamic configuration of tethered balloons is more or less standard. A typical machine [2-4] looks like a teardrop-shaped (blimp-shaped) balloon with fins, to which a gondola with the payload is attached. The lift of such aerostat depends only on its size, and does not depend on the velocity of the wind, at the same time, the resistance force grows proportionally to the square of the velocity of wind. For a fixed length of a tether, the force of resistance tends to reduce the height of the machine's flight. The capability of the aerostats to retain the height regardless of the wind depends on their size: the larger is the volume of the balloon, the less sensitive is the aerostat to the force of the wind. Extra-large aerostats (with the volume of the order of tens of thousands of cubic meters) are practically independent of any weather [5]. However, for a lot of tasks, cheap low-sized TASs are quite sufficient, with the balloon volume of about 10 $m^3$.
One of the ways to improve the operational characteristics of TAS, is to use a hybrid design, when the machine bears wings. They create additional lift that strengthens the machine's steadiness against the wind.
A classical tethered aerostat maintains steady course and pitch parameters due to its tail fins, and does not need a system of control. In a hybrid design, a system of control and stabilizing is required, in order to fully realize its advantages. This paper examines a design of a low-sized TAS, presents its aerodynamic characteristics and describes the structure and the operation logic of the automatic onboard control system.

## The requirements to the aerodynamic configuration of the TAS.

The TAS we are devising is intended for meteorology observations. According to the technical project, the machine is to be capable of flying at the height up to 1000 m, has to have the construction's weight not heavier than 7 kg and the weight of the target equipment must not exceed 2.5 kg. To ensure the required accuracy of the conducted observations, the machine has to be stabilized relative to the horizon, so that the angles of pitch and bank would not exceed 1° ($|\vartheta| \le 1°$, $|\gamma| \le 1°$). Let us see, how all those requirements affect the aerodynamic configuration of the machine.
In order to have the minimal effect on the angle of pitch by a change in the angle of attack (the latter being caused by upward or downward air currents), the machine's steadiness in the pitch axis has to be close to neutral ($m_z^\alpha \approx 0$). Since the angular evolutions of the machine take place as relevant to the hinge, by which the tether cable is attached to the glider, by varying the distance to the hinge from the nose of the fuselage $x_t$, we can eventually discover the necessary amount of reserve in the longitudinal steadiness of the machine $m_z^\alpha$.
The machine has to have static steadiness of its course relative to the point of the tether attachment ($m_y^\beta < 0$), which would ensure a constant orientation of the machine with its nose against the wind, and, accordingly, would provide the proper operating conditions for the measurement equipment.

The aerostatic balloon has to have the volume that is minimally required to elevate the machine along with the cable to the operational height in the absence of wind. Otherwise, the larger sizes of the balloon will cause an undesirable increase in the load on the structure and in weight.
The wing should provide the lift that is sufficient for maintaining the altitude of flight, taking into account the effect of the wind on the machine and on the tether cable.

**The description of the aerodynamic profile.**
The hybrid aerostat can be constructed according to different aerodynamic profiles, for example, it can be a thick wing, filled by a buoyant gas, or a it can be a balloon, close to a sphere in shape, combined with a flat fabric wing [6-9]. Based on configuration reasons, the aerodynamic profile represented in Fig. 1. was chosen.

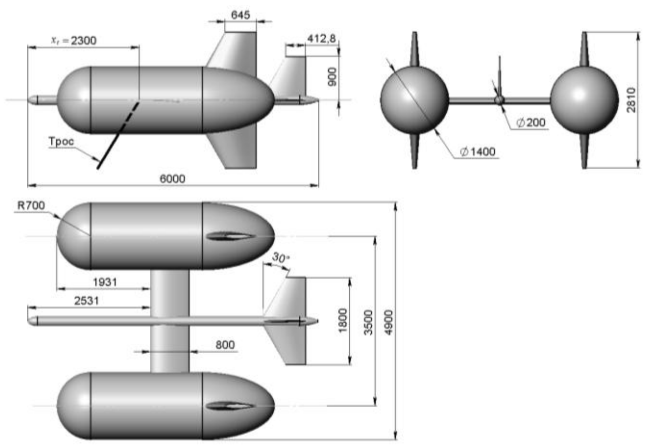


**Figure 1 – The aerodynamic profile of the TAS.**

The aerostatic lift is created by two balloons on each side that have the shape of the solids of revolution.
The wing is represented on the projection as rectangular, its profile is constant in span, which ensures a maximally technological approach. At the stage of initial elaboration, the low-speed profile FX63-137 was chosen for the wing. Its asymmetrical form allows to gain lift at the zero angle of attack. The wing's chord is quite large, and has minor elongation, respectively, ( $\lambda = 2.6$ ), which provides its high durability and flexural and twist rigidity, while keeping the weight of the construction minimal.
The bank of the machine is controlled by means of the ailerons, placed along the entire trailing edge of the wing, that have a chord of 200 mm.
The fuselage is made in the form of a tube of a round cross section, relatively small in diameter, since the size of the equipment, placed inside it, is relatively small. The substantial extent of the fuselage is caused by the necessity to have the measurement equipment installed in the front, so that the balloons should not influence the measured parameters (the velocity of the current and the air pressure). The tail fins are installed in the rear part to provide due efficiency.
The all–moving stabilizers take the function of the elevation rudder (ER). This provides the maximum effectiveness of the rudder and simplifies its design, in comparison with the classical, for the subsonic configurations, type, when the elevation rudder is the deflected trailing edge of the stabilizer.
In the tail part of the fuselage, a keel is installed. Since there are no explicit requirements to the control and stabilizing of the machine's course, the direction rudder is missing. However, it can be added after test flights and after defining the real degree of perturbations that affect the machine. To increase the steadiness on the course, while retaining the minimal weight of the construction, the balloons have inflated keels.
The aerodynamic characteristics of the machine were computed by utilizing the implicit method for the numerical solution of the Navier-Stocks equations, the latter averaged by the Reynolds method, implemented in the software package ANSYS CFX. While carrying out the calculations, the guidelines were applied, as set out in the works [10-13]. The computational grid contained about 60 million cells. The calculations presumed a stationary setting, the environment was considered to be incompressible, the SST model of turbulence was applied [14]. The momentums of pitch and course were computed relative to the nose of the fuselage. The obtained aerodynamic characteristics are represented in Figures 2-6.
The aerodynamic lift increases with the growth of the velocity of wind and of the angle of attack, and can by far exceed the weight of the machine (Fig. 2). As it was noted above, this is necessary for the accessible aerodynamic quality of the system "the machine+the cable".
The influence of the tether on the aerodynamic quality (its maximal length equal to 1 km) has been estimated roughly by means of the additional component in calculating the resistance of the machine: $\Delta C_{xa} = Cx_{cable} \cdot d \cdot L / S$, where $Cx_{cable} = 1$ – the resistance coefficient of the round cylinder [15], $d = 2$ mm и $L = 1$ km – the diameter and the length of the cable, $S = 2.1$ m² – the characteristic area necessary for calculating the resistance coefficient. Admitting that the cable has the form of a straight line, let us define the angle between the cable and the horizon: $\varphi = arctg(K)$. If the flight height is low, which allows to neglect the cable's influence, the maximal aerodynamic quality of the machine amounts 5.8 (Fig. 3), and the functional dependence $\varphi(\alpha)$ within the range $0 \le \alpha \le 20°$ has a "shelf" $\varphi \approx 80°$ (the machine is practically hovering above the site of launch). The increase in the length of the cable up to 1 km causes a decrease in the aerodynamic quality and in the angle $\varphi$ (Fig. 3-4), however, the machine is capable of continuing the flight at a lower altitude (providing the length of the cable does not change). The "minus" values of the angle of attack cause a sharp decrease in the angle $\varphi$, therefore, if the length of the cable is fixed, the machine will be going down with the simultaneous decrease in the angle of attack. At $\alpha \le 5°$, the tether will take the horizontal position ($\varphi = 0°$) and the machine will not be able to continue the flight (Fig. 4). Which means, that the machine should carry a system of control onboard, for maintaining the angle of attack within the range that provides safe flight.

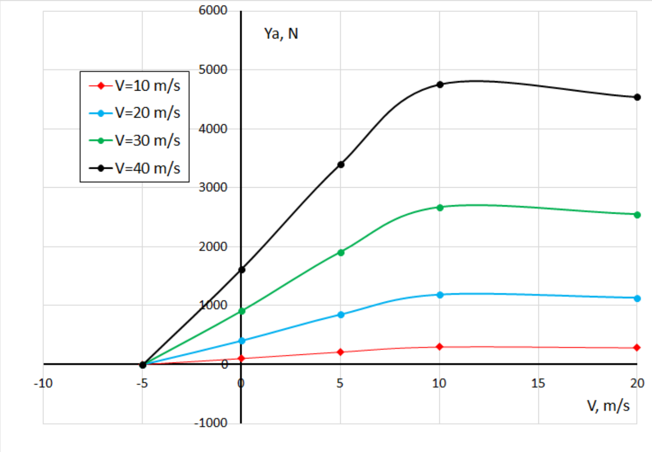


**Figure 2 – The dependency of the glider's lift on the angle of attack and the velocity of wind (H=0 m).**

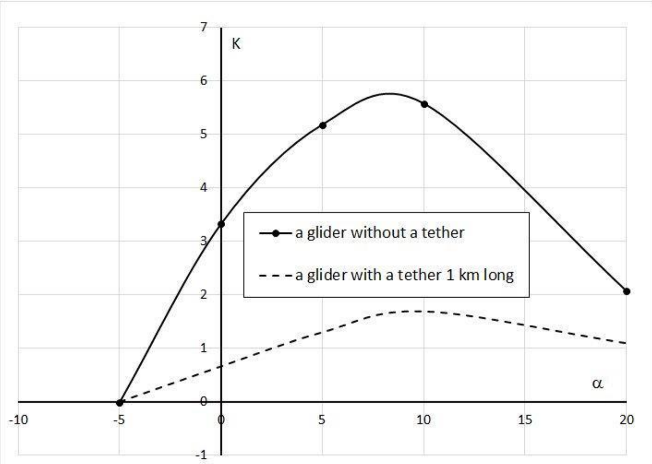


**Figure 3 – The dependency of the aerodynamic quality on the angle of attack.**

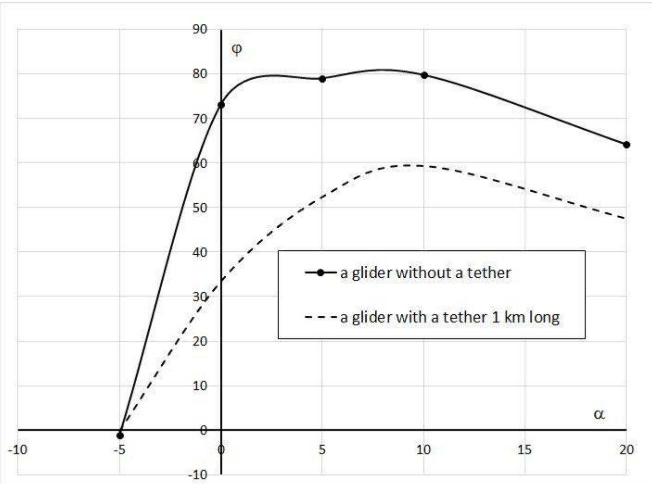


**Figure 4 – The dependency of the angle of the cable's lean to the horizon on the angle of attack.**

The selection process of the attachment point of the cable to the machine is shown in Fig. 5-6. Making the distance from the nose of the fuselage to the attachment point of the cable larger, causes a decrease in the static steadiness of the machine along the axes of pitch and course. At $x_t \approx 2.3$ m, the machine remains steady in the course $(m_y^{\beta} < 0)$ and neutral in the pitch $(m_z^{\alpha} \approx 0)$, therefore, the machine will only be responding to the change of the wind direction in the horizontal plane. The change in the angle of attack will not have a considerable effect on the orientation of the machine in the vertical plane.

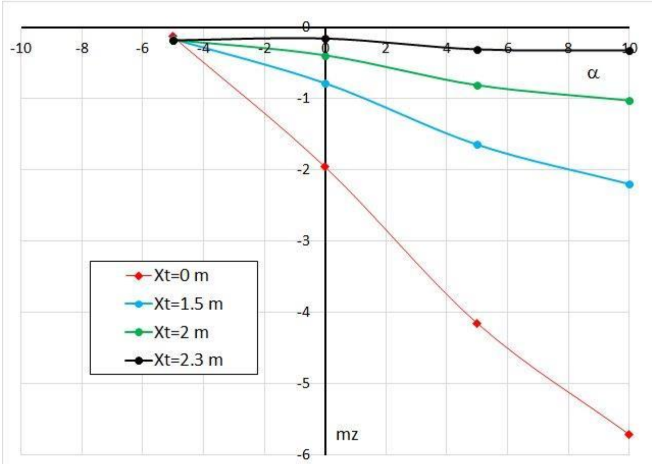


**Figure 5 – The dependency of the coefficient of the pitch momentum on the position of the point of the cable's attachment ($S_{char}$=2.1 m² and b=1 m).**

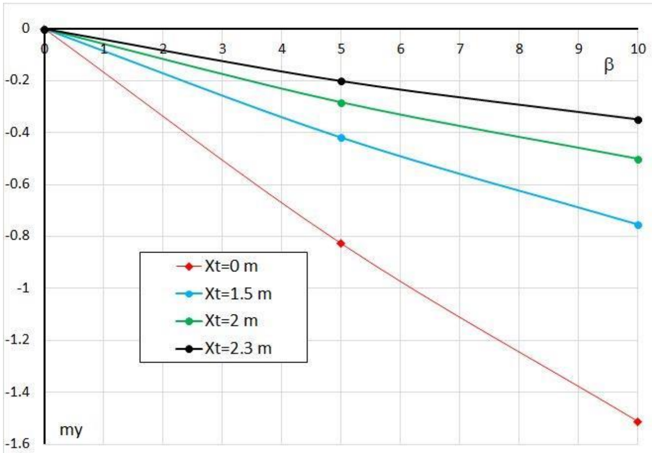


**Figure 6 – The dependency of the coefficient of the yaw momentum on the position of the point the cable's attachment ($S_{char}$=2.1 m² and L=2.1 m).**

**The mathematical model for computing the parameters of the TAS's motion.**

In order to compute the trajectories of the machine's motion, depending on the velocity and direction of wind, with the work of the system of control and stabilizing taken in regard, a mathematical model was devised accordingly. It is based on differential equations that describe the dynamics of a flying machine [16].

The machine is regarded as an object of control, that consists of several modules, that have their input and output channels and the algorithms of realization, that reflect its operation (Fig. 7).

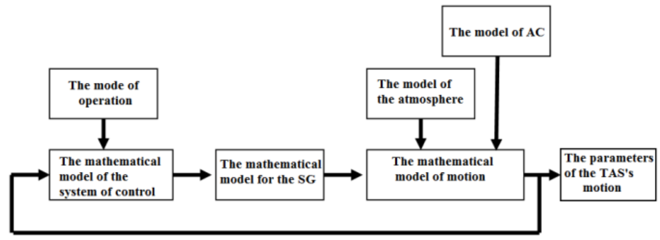


**Figure 7 – The modular scheme of the mathematical model for computing the parameters of motion.**

Let us consider the building blocks of the mathematical model.

**The model of the atmosphere.**
The aerodynamic and aerostatic forces, that affect a flying machine's performance, depend on the atmospheric parameters – its density, pressure and the temperature of the air. These parameters, in turn, are determined by the altitude of flight, by the geographic latitude, by the time of the year and day, and by a number of other factors. The mathematical model of the atmospheric parameters is a set of dependencies in formulae that approximate the values from the tables [17], a set where the altitude above the sea level and the seasonal specifics are taken as input, and the output consists of the temperature, the air density, and besides, of the value of the acceleration of gravity.

**The model of aerodynamic coefficients**.
The subprogram for computing the aerodynamic coefficients (AC) of the machine, depending on the flight conditions, is addressed to at each cycle of the process of computing of the parameters of movement. To compute the AC, the formulae are utilized that approximate the calculated values of the AC, obtained from numeric calculations, depending on the angles of attack, of glide, and on other parameters.

**The mathematical model of the steering gear.**
The steering gear (SG), which manipulates the controls of the machine in compliance with the autopilot's commands, is a complex closed-loop automated system. The SG affects the dynamics of the system and cannot be regarded as an inertia-free element of the system of control. At the initial stage of designing, the mathematical model of the SG is set down as an aperiodic link of the first order:

$$W_{SG} = \frac{1}{0.04p + 1} \qquad (1)$$

At the following stages of work, according to the results of experimental testing of the gear, its model can be further elaborated.

**The mathematical model of the control system** (CS) is intended for changing the operating condition of the machine according to the laws of management. The CS has two modes of operation:

- the mode of stabilizing the angular position of the machine relative to the horizon;
- the mode of stabilizing the height.

The algorithm of control in the mode of stabilizing the angular position of the machine as relative to the horizon, in the vertical and horizontal planes, is based on the proportional-integrating-and-differentiating regulator (PID-regulator). The PID-regulator forms a control signal, which is a sum of three components, the first one is proportional to the difference between the input and the feedback signals (the signal of synchro error), the second is the integral of the synchro error signal, and the third is the derivative of the synchro error signal:

$$u(t) = Kp \cdot e(t) + Ki \int_0^t e(t) \cdot dt + Kd \frac{de}{dt} \qquad (2)$$

where $Kp, Ki, Kd$ are the coefficients of intensifying of the proportional, integrating and differentiating components of the regulator, respectively;
$e(t)$ – the synchro error signal;
$e(t) = \vartheta$ (in the law of control over the vertical axis);
$e(t) = \gamma$ (in the law of control over the horizontal axis);
$\vartheta, \gamma$ – the angles of pitch and bank of the machine, respectively;
$u(t)$ – the output signal.

The mode of stabilizing the altitude is turned on in order to prevent significant variations of the parameter of height, caused by a vertical component of the velocity of wind. At that time, the law of control with the feedback on the rate of the change in height starts to work. For instance, in a downward current, when the machine begins to loose height, after the height stabilizing mode is turned on, the CS sends a signal to deflect the elevation rudders, in order to obtain nose-up pitching, and the angle of the pitch begins to increase, until the moment when the loss of the flight height finishes.
If an upward air current of significant power arises (that is, at wide "plus" angles of attack) the aerodynamic force of a flying machine can cause the cable breakage. The system of control in the mode of "stabilizing the height" decreases the angle of attack, deflecting the elevation rudder for the nose-down diving.

**The interaction of the machine and the tether.**
Within the framework of the devised mathematical model of the machine's motion, the tether (cable) is regarded as linearly elastic and capable of damping.
The coefficient of energy dissipation is estimated by the following formulae:

$$\begin{cases} F_T = k_R \cdot \Delta l^2, when \Delta l \to \Delta l_{\max} \\ F_T = \dfrac{k_R}{3} \cdot \Delta l^2, when \Delta l \to 0 \end{cases} \qquad (3)$$

where $k_R$ – the coefficient of rigidity. For the chosen cable, by means of the known characteristics: $\Delta l$ = 5%, when the tearing force $F_{tear}$ = 120 kg, we can define the coefficient of rigidity $k_R = F_{TEAR} / \Delta l$ =24 kN/m.
In the process of the machine's motion, such situations can occur that the cable from strained becomes lax, it is then exposed to dynamic load (a yank). At that moment, the kinetic energy of the machine

$$E = \frac{mV^2}{2} \qquad (4)$$

is converted into the potential energy of the stretched cable

$$U = k_R \cdot \frac{\Delta l^2}{2} \quad (5)$$

and, therefore, putting down the equation E=U, we will get the maximal permissible value of the strain $F_T = \sqrt{k_R \cdot m \cdot V^2}$ , that the cable receives from the machine, the cable’s damping qualities not taken into account.
The same formula allows to define the value of the machine's speed, which, if exceeded, will cause the cable's breakage:

$$V_{\max} = \sqrt{\frac{F_T^2}{k_R \cdot m}} \quad (6)$$

For the taken mechanical characteristics of the cable with the length $l_{presc}$=1000 m, the limit of the machine's own speed, that would cause the elongation of the cable, will amount $V_{\max} = 77$ m/s, and with the length $l_{presc}$=100 m, the speed limit will amount $V_{\max} = 30$м/с.
In case the cable is strained, the tearing force $F_T$ will be determined by the aerodynamic forces affecting the machine:

$$F_T = \sqrt{X_g^2 + Y_g^2 + Z_g^2} \quad (7)$$

**The equations of the machine's motion**
The layout of the forces, that affect the machine’s center of gravity, while flying in the horizontal plane, is shown in Fig. 8.

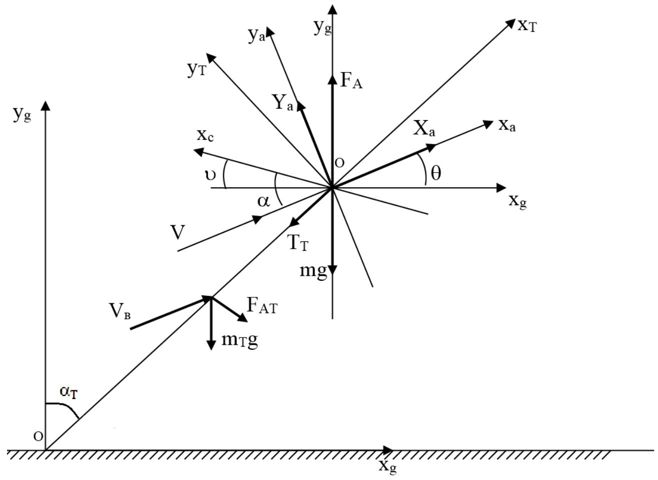


**Figure 8 – The layout of forces, that affect the TAS.**

The notation in Figure 8:
Fa – the summative aerostatic lift;
Ya – the aerodynamic lift;
Xa – the force of the head-on resistance;
V – the speed of the machine's center of gravity relative to the air (in the absence of wind – relative to the surface of the Earth;
$T_T$ – the force of the mechanical impact from the cable (tether);
$F_{AT}$ – the aerodynamic force, affecting the cable (tether);
m – the weight of the machine;
$m_T$ – the weight of the cable (tether);
g – the acceleration of gravity;
$\alpha_T = 90° - \varphi$ – the angle of the cable's lean;
□ – the angle of attack;
□ – the angle of the trajectory's lean to the horizon.

The equations, that describe the machine's motion:

$$\dot{V}xg = \frac{Fxg}{m} \quad (8)$$

$$\dot{V}yg = \frac{Fyg}{m} \quad (9)$$

$$Vg = \sqrt{Vxg^2 + Vyg^2} \quad (10)$$

$$Fxg = Fxa \cdot \cos\theta - Fya \cdot \sin\theta + F_{AT}^{Xg} - T_T^{Xg} \quad (11)$$

$$Fyg = Fya \cdot \cos\theta + Fxa \cdot \sin\theta - (m + m_T) \cdot g + F_A + F_{AT}^{Yg} - T_T^{Yg} \quad (12)$$

$$Fxa = -Cxa \cdot Q \cdot S \quad (13)$$

$$Fya = Cya \cdot Q \cdot S \quad (14)$$

$$F_{AT}^{Xg} = 0.25 \cdot (\rho_h \cdot V_n^2 \cdot D_T \cdot L_T) \cdot \cos a_T \quad (15)$$

$$F_{AT}^{Yg} = 0.25 \cdot (\rho_h \cdot V_n^2 \cdot D_T \cdot L_T) \cdot \sin a_T \quad (16)$$

$$F_A = 2 \cdot g \cdot Vb \cdot (\rho_h - \rho_{He}) \quad (17)$$

$$T_T^{Yg} = T_T \cdot \sin a_T \quad (18)$$

$$T_T^{Xg} = T_T \cdot \cos a_T \quad (19)$$

$$m_T = 0.002 \cdot L_T \quad (20)$$

$$V_n = V_B \cdot \cos(a_T - \theta) \quad (21)$$

$$\begin{cases} T_T = K_{jT} \cdot \Delta L_T \; when \frac{d\Delta L_T}{dt} > 0 \\ T_T = \frac{1}{3} K_{jT} \cdot \Delta L_T \; when \frac{d\Delta L_T}{dt} < 0 \\ T_T = 0 when \frac{d\Delta L_T}{dt} = 0 \end{cases} \quad (22)$$

$$Q = 0.5 \cdot \rho_h \cdot V^2 \quad (23)$$

$$\begin{cases} \theta = 90^0 & when V_w xg = 0, V_w yg > 0 \\ \theta = -arctg(\frac{V_w yg}{V_w xg}) & when\ V_w xg > 0, V_w yg > 0 \\ \theta = arctg(\frac{V_w yg}{V_w xg}) + 180^0 & when\ V_w xg < 0, V_w yg > 0 \end{cases} \quad (24)$$

$$\begin{cases} \theta = -90^0 & when V_w xg = 0, V_w yg < 0 \\ \theta = -arctg(\frac{V_w yg}{V_B xg}) & when V_w xg > 0, V_w yg < 0 \\ \theta = -arctg(\frac{V_w yg}{V_w xg}) - 180^0 & when\ V_w xg < 0, V_w yg < 0 \end{cases} \quad (25)$$

$$\begin{cases} a_T = 90^0 & when Yg = 0 \\ a_T = arctg(\dfrac{Xg}{Yg}) & when\, Yg > 0 \end{cases} \quad (26)$$

$$L_T = \sqrt{Xg^2 + Yg^2} \quad (27)$$

S – the characteristic area;

$D_T, L_T$ – the diameter and the length of the cable, respectively;

$Vb$ – the volume of the balloon;

$\rho_h$ и $\rho_{He}$ – the air density at the altitude and the gas density in the balloons, respectively.

In a generalized case, the system for stabilizing the spatial motion of a flying machine, from the mathematical point of view, is described by a set of non-linear differential equations and non-linear functional dependencies.

The system for stabilizing the spatial motion of a flying machine consists of an object of regulating and a regulator. The object of regulating is described by the following system of differential equations (they are the equations of short-periodic motion) [16]:

$$\frac{d\alpha}{dt} = \omega_{z1} - a_4\alpha - a_5\delta_E \quad (28)$$

$$\frac{d\omega_{z1}}{dt} = a_2\alpha + a_1\omega_{z1} + a_3\delta_E \quad (29)$$

$$\frac{d\vartheta}{dt} = \omega_{z1} \quad (30)$$

where the notation stands for:

- $a, J, d_E$ – the angles of attack, pitch and deflection of the elevation rudders, respectively;
- $\omega_{z1}$ – the angular speed of the object in the relevant coordinate system;
- *a1, a2, a3, a4, a5* – dynamic coefficients of the longitudinal motion of the object of regulating.

The system of differential equations represents a linearized mathematical model of perturbed motion of a flying machine, as compared to the mode of an undisturbed stabilized state.

Introducing the following notation:

$$A = \frac{qs}{mV}, \quad B = \frac{qsL}{J_{x1}}, \quad C = \frac{qSL}{J_{y1}}, \quad D = \frac{qSb_a}{J_{z1}} \quad (31)$$

we obtain dynamic coefficients from the following interrelationships:

$$a_1 = D\frac{b_a}{V}(m_{z1}^{\bar{\omega}z1} + m_{z1}^{\dot{\alpha}}) \quad (32)$$

$$a_2 = Dm_{z1}^{\alpha} \quad (33)$$

$$a_3 = Dm_{z1}^{d_E} \quad (34)$$

$$a_4 = AC_y^{\alpha} \quad (35)$$

$$a_5 = AC_y^{d_E} \quad (36)$$

where the notation stands for:

- L, S, $b_a$ – the characteristic dimensions to which the aerodynamic coefficients are reduced;
- V, q – the airspeed of a flying machine and the speed thrust;
- Jx1, Jy1, Jz1 – the inertial characteristics of a flying machine;
- m – the weight of a flying machine;
- $C_y^{\alpha}, m_{z1}^{\alpha}, C_y^{\delta_E}, m_{z1}^{\delta_E}, m_{z1}^{\bar{\omega}z1}, m_{z1}^{\dot{\alpha}}$ – the partial derivatives of the aerodynamic coefficients of a flying machine as regards the angle of attack, angle of deflection of the elevation rudder, the angular rate of the pitch and the rate with which the angle of attack is changing, respectively.

The object of regulating can be represented through symbolic operators:

$$p\alpha = \omega_{z1} - a_4\alpha - a_5\delta_E; \quad p\omega_{z1} = a_2\alpha + a_1\omega_{z1} + a_3\delta_E; \quad p\vartheta = \omega_{z1}. \quad (37)$$

The solution of the equations of the machine's motion was implemented through creating a program in Visual Basic 6.0. The user has the options of entering the initial conditions of the launch, of inputting the changes in the characteristics of geometry, weigh-inertia and center of gravity position, of setting the values for the gear ratio of the control system, of inputting the characteristics of the cable and the wind loads. Such set of data gives the opportunity to an engineer, to carry out theoretical calculations in search of the optimal parameters of motion, and is caused by the necessity of specifying the machine's parameters at further stages of work.

In the process of running the program, a file is created with the results of a simulation, that can be used for plotting graphs and conducting analysis by means of analytical graphs.

**The results of a computer simulation.**

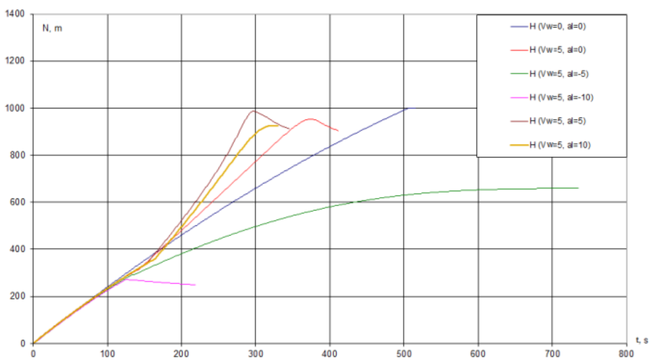


**Figure 9 – The change of the machine's altitude depending on the velocity ($V_W$=0, $V_W$=5 m/s) and direction (al, degrees) of the wind.**

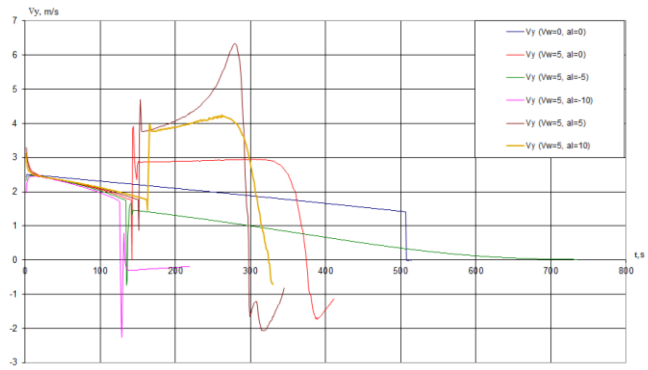


**Figure 10 – The change of the vertical component of the machine's speed depending on the velocity (Vw=0, Vw=5 m/s) and direction of the wind (al, degrees).**

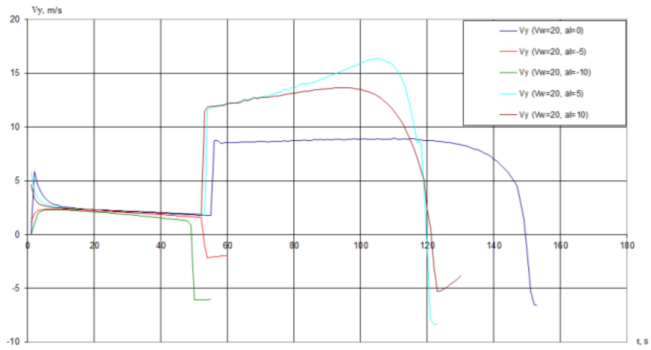


**Figure 13 – The changes of the vertical component of the machine's speed depending on the velocity (Vw=20 m/s) and direction (al, degrees) of the wind.**

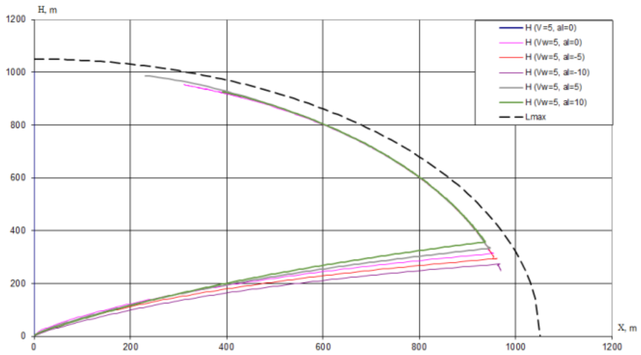


**Figure 11 – The profile of the machine's elevation in the vertical plane depending on the velocity (Vw=0, Vw=5 m/s) and direction of the wind (al, degrees).**

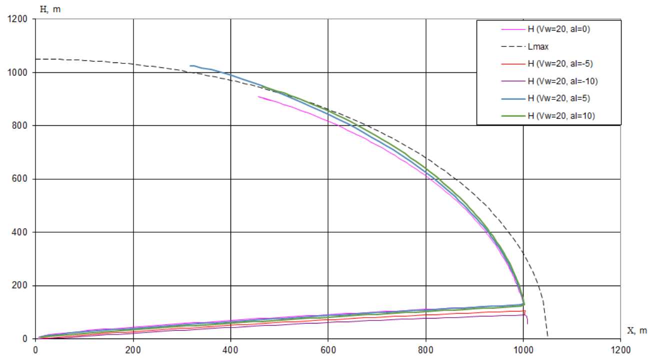


**Figure 14 – The profile of the machine's elevation in the vertical plane depending on the velocity (Vw=0, Vw=20 m/s) and direction (al, degrees) of the wind.**

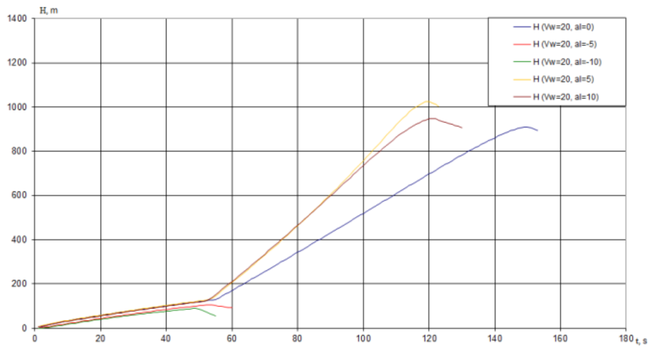


**Figure 12 – The changes of the machine's altitude depending on the velocity (Vw=20 m/s) and direction (al, degrees) of the wind.**

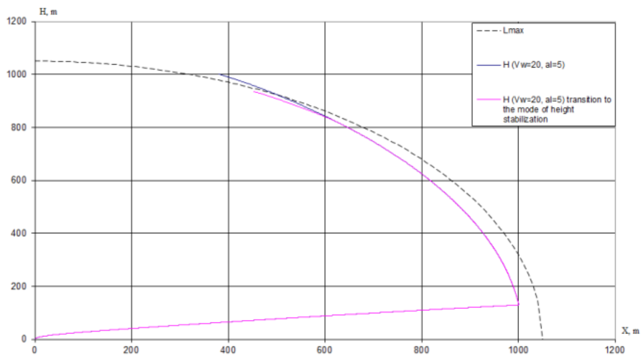


**Figure 15 – The profile of the machine's elevation at the velocity of the wind 20 m/s and the wind's direction $\alpha = 5°$, with the transition into the height stabilizing mode.**

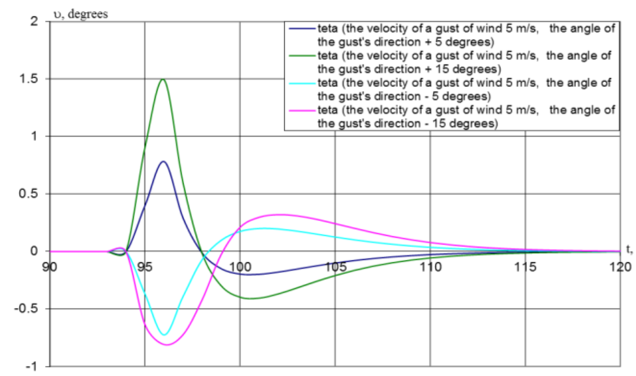


**Figure 16 – The machine's response to a gust of wind (H=1000 m, $V_W$=10 m/s).**

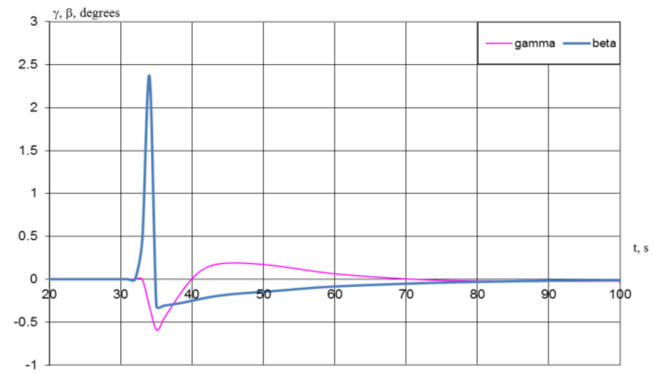


**Figure 17 – The machine's response to a gust of wind (H=100 m, $V_w$=10 m/s)**

Figures 9-17 show the parameters of the machine's motion, that demonstrate the transition to a maximal altitude, limited by the length of the tether, under various types of the wind's disturbance. In all elevation modes, no limitations on the flying machine's motion to do with the velocity of the cable's unwinding were presumed.

As can be seen in Figures 9-12, in the absence of wind, the machine climbs to the prescribed altitude ($H_{presc}$=1000 m) in 500 c with the average vertical speed of 2 m/s. If there is a vertical component in the wind, due to the appearance of an upward current, the time of elevation to the prescribed altitude varies, and lies within the range of 120...400 s. If there is a vertical component in the wind due to a downward current, the climb to the prescribed altitude does not appear possible, while maintaining the mode of stabilizing the angular position of the machine, relative to the horizon. In order to execute climb in these conditions, the machine is to be switched into the mode of stabilizing the pre-programmed angle of the pitch (Fig. 18, at 120 sec the mode of stabilizing height by means of the pre-programmed angle of the pitch was engaged).

In Figures 11 and 14, the profiles of a flying machine's elevation in the vertical plane are demonstrated. As can be seen from the figures, at the wind velocity of 20 m/s and a "plus" angle of attack, the flying machine's impact upon the tether exceeds the maximal permissible load.

In Fig.15, a comparative chart of the machine's motion is shown, with engaging the height stabilizing mode, in order to prevent the tether's breakage.

In Fig. 17, the transitional processes are shown that take place in the pitch axis, depending on the angle of direction of a gust of wind.

For the chosen design of the machine, there are limitations, as to the permissible range of its application with regard to speed – from 0 to 20 m/s, determined by the permissible load over the tether.

To lessen the dynamic load, that comes from the cable's strain, it is reasonable to limit the speed of the flying machine's elevation by limiting the velocity of the cable's unwinding.

## Conclusions

1. The aerodynamic configuration of a low-sized tethered aerostat has been designed, the one capable of performing flight at height up to 1000 m. The computable aerodynamic characteristics were defined, within the ranges of $-5° \le \alpha \le 20°$, $-10° \le \beta \le 10°$. For the tether, the proper point of attachment to the fuselage was selected, that should provide the required degree of longitudinal and lateral steadiness.
2. The mathematical model of the control system has been devised, that includes the algorithms of control and stabilizing.
3. A simulation of the machine's dynamics in the longitudinal and lateral axes has been carried out. It was shown, that the control system provides the stabilization of the angular position as regards the angles of pitch and bank with the required precision, in the range of the wind's velocity up to 20 m/s. In order to prevent the unacceptable loss of height at "minus" angles of attack, the height stabilizing mode is engaged.
4. The article has been prepared within the framework of conducting applied scientific research and experimental projects (ASREP) according to Agreement No. 14.579.21.0082 on providing a grant, with the financial help from the Ministry of science and education of the Russian Federation. The unique identifier of ASREP is RFMEFI57914X0082.

## References

1. Bendin, S. (n.d.). *Aerostats will be providing the surveillance over the air borders of the USA and Israel.* Retrieved June 28, 2015, from http://www.pandia.ru/text/77/408/43817.php.
2. *The official site of the "Lockheed-Martin" company.* (n.d.). Retrieved on June 28, 2015, from www.lockheedmartin.com/us/products/lighter-than-air-vehicles.html.
3. *The official site of the "TCOM L.P. " company.* (n.d.). Retrieved June 28, 2015, from http://www.tcomlp.com/aerostat-platforms.
4. *The official site of the Closed Joint-Stock company "The aeronautic center "Avgurr".* (n.d.). Retrieved June 28, 2015, from http://rosaerosystems.ru.
5. Verba, G., Shugarev, S., Ivchenko, B., Ponomarev, P., & Talesnikov, M. (2012). The modern world trends in designing aeronautic machines for the benefit of law enforcement agencies. *The Herald of the South Federal University (in technical sciences), 3*, 49-588.

6. *A tethered balloon. Patent of the Russian Federation No. 40289 for a useful model.* (2004, September 10).
7. *A tethered balloon, steady under the action of wind. Patent No. 2279994 of the Russian Federation.* (2006, July 20). No. 2004139144/11; applied on 22.12.2004.
8. *A hybrid flying machine. Patent of the Russian Federation No. 109738 for a useful model.* (2011, October 27).
9. *The kytoon "Colibri".* (n.d.). The site of the Moscow Aviation Institute. Retrieved June 28, 2015, from http://www.mai.ru/science/dev/index.php?ELEMENT_ID=9897.
10. Bosnyakoff, S., Akinfiev, V., Vlasenko, V., Glazkov, S., Lysenkoff, A., Matyash, S., & Michaylov, S. (2006). The methodology of mathematical modelling of the streamlining of models in aerodynamic tubes, and the experience of its application. *The machines of the airfleet*, *5*, 1-20.
11. Bosnyakoff, S., Akinfiev, V., Vlasenko, V., Glazkov, S., Lysenkoff, A., Matyash, S., & Michaylov, S. (2006). The methodology of mathematical modelling of the streamlining of models in aerodynamic tubes, and the experience of its application. *The machines of the airfleet*, *6*, 1-13.
12. Tarasenko, A. (2009). The practical aspects of solving the tasks of the outer aerodynamics of the subsonic flying machines within the frames of Euler's equations. *The machines of the airfleet*, *1*, 22-44.
13. Tarasenko, A. (2009). The practical aspects of solving the tasks of the outer aerodynamics of the subsonic flying machines within the frames of Reynolds equations. *The machines of the airfleet*, *2*, 1-16.
14. Menter, F. (1994). Two-equation eddy viscosity turbulence models for engineering applications. *AIAA Journal*, 8(32), 1598-1605.
15. Devnin, S. (1983). *The aero- and hydromechanics of constructions with bad streamlining: a reference book.* Leningrad: Shipbuilding.
16. Lebedev, A., & Chernobrovkin, L. (1973). The flight dynamics of pilotless flying machines. Moscow: Mechanical engineering.
17. *GOST 4401-81. The standard atmosphere: the parameters.* (2004). Moscow: The standards publishing house.